

1 **A continental-wide decline of occupancy and diversity in five charismatic** 2 **Neotropical carnivores**

3
4 **Florencia Grattarola^{1,*}, Kateřina Tschernosterová¹, Petr Keil¹**

5
6 ¹ Faculty of Environmental Sciences, Czech University of Life Sciences Prague, Kamýcká 129,
7 Praha – Suchbátka, 16500, Czech Republic

8 * Corresponding author (flograttarola@gmail.com)

9 10 **Abstract**

11 The Neotropics are a global biodiversity hotspot that has undergone dramatic land use changes
12 over the last decades. However, a temporal perspective on the continental-wide distributions of
13 species in this region is still missing. To unveil it, we model the entire area of occupancy of five
14 Neotropical carnivore species at two time periods (2000-2013 and 2014-2021) using integrated
15 species distribution models (ISDMs) in a Bayesian framework. The carnivores are the jaguarundi
16 (*Herpailurus yagouaroundi*), margay (*Leopardus wiedii*), maned wolf (*Chrysocyon brachyurus*),
17 tayra (*Eira barbara*), and giant otter (*Pteronura brasiliensis*). We mapped the temporal change,
18 the areas where gains and losses accumulated for all species (hotspots of change) and calculated
19 the spatial and temporal dissimilarity. We show that most carnivore species have declined their
20 area of occupancy in the last two decades, that diversity has decreased over time, and that species
21 composition has diverged (i.e., dissimilarity among assemblages increased). By looking at
22 different facets of biodiversity simultaneously, we revealed that the ongoing changes in land use

23 in the Neotropical region have been coupled with a transformation in the status of biodiversity
24 there.

25

26 **Keywords:** biodiversity change, geographic range, dynamic patterns, hotspots of change,
27 integrated species distribution models, Bayesian, species richness.

28

29 **1 Introduction**

30 The Neotropics are biologically megadiverse (Grenyer et al., 2006; Raven et al., 2020) but also
31 face one of the most significant degradations of natural areas (Barlow et al., 2018; WWF, 2020).

32 The main land transformations are related to converting native grasslands and forests into
33 farming lands (e.g., soybean plantations), pastures for cattle ranching, and exotic-tree forestry
34 (Baeza et al., 2022; Curtis et al., 2018; Pompeu et al., 2023; Song et al., 2021; Souza et al.,
35 2020). Likely as a consequence, there have been reports of defaunation in the Neotropics
36 (Bogoni et al., 2020; Emer et al., 2019; Magioli et al., 2021). While these studies have
37 contributed valuable insights, they are either geographically limited in their extent (e.g., local to
38 the Atlantic forest, Emer et al., 2019, or Caatinga, Moura, Oliveira, et al., 2023), temporally too
39 broad (e.g., comparing current distributions with late Quaternary periods, Sandom et al., 2014),
40 or they rely on forecasts or hindcasts rather than on direct empirical comparisons (e.g., using
41 IUCN range maps, Bogoni et al., 2020). A data-driven study with a continental extent that aligns
42 with the recent degradation of natural areas (i.e., last 20 years) is missing.

43

44 At the large continental extent, a fundamental property of a species is its geographical
45 range (Brown et al., 1996): the set of limits to the spatial distribution of a species (e.g.,

46 boundaries within which a species occurs) (Gaston, 2003). We can stack ranges of multiple
47 species to get continental maps of species diversity (Mittermeier et al., 2011; Myers et al., 2000;
48 Roll et al., 2017), and we can use them to study the differentiation of species composition, the
49 so-called beta diversity (Anderson et al., 2011; Koleff et al., 2003). A joint knowledge of these
50 properties (i.e., species ranges, species diversity, and beta diversity) gives a holistic picture of the
51 state of nature at large scales. While a map of species richness can show biodiversity hotspots,
52 considering it jointly with the identity and area of occupancy of each species can reveal centres
53 of endemism, as well as areas with unique species composition. In the Neotropics, at the
54 resolution of 100 x 100 km, species ranges for vertebrates have long been available (Schipper et
55 al., 2008) and analysed (Coelho et al., 2023). The problem is that all of this is completely static.
56 We still don't know how it all changes in time, even though the knowledge of the temporal
57 dynamics of species' occupancy (are species expanding or shrinking?), diversity (are sites losing
58 or gaining species?), and beta diversity (is there biotic homogenisation or differentiation?) is
59 potentially critical in the face of the ongoing land transformation in the Neotropics.

60

61 The main reason for the lack of knowledge about continental-wide temporal dynamics is
62 the amount and quality of data in the region (Hortal et al., 2015). Datasets collected/observed at
63 the same location at different points in time over large spatial extents, such as national gridded
64 atlases, are practically non-existent. This is a cross-cutting issue, as it limits our capacity to
65 address the biodiversity knowledge gap, identify threats to biodiversity, and take evidence-based
66 decisions and actions.

67 Data about species distribution come in three forms (Kissling et al., 2018):

68 1. First, presence-only point occurrences are the most common type of observation
69 data. Contributing these using smartphones through community science initiatives has become
70 popular in the region (Pocock et al., 2018). The iNaturalist initiative, for instance, has nine
71 national sites in the region (Mexico, Guatemala, Costa Rica, Panama, Colombia, Ecuador, Chile,
72 Argentina, and Uruguay). The point occurrences that this platform hosts are of particular
73 importance in such an under-sampled region, as they often cover a larger portion of area than
74 structured survey data. However, incidental presence-only observations are usually spatially,
75 temporally, and taxonomically biased (Oliveira et al., 2016).

76 2. Second, high-quality biodiversity data, for which we know the exact sampling
77 effort and methods and where both species' presences and absences are recorded, are rarely
78 shared through the GBIF initiative. Examples are data from camera traps (Steenweg et al., 2017),
79 whose use in Latin America is increasing rapidly (Delisle et al., 2021). Despite previous efforts
80 to collate camera trap surveys in the region (Ahumada et al., 2011), plenty of heterogeneous data
81 still can be mobilised (Kühl et al., 2020; Scotson et al., 2017).

82 3. Third, expert range maps (IUCN, 2023) are a major data source for
83 macroecological studies in this region. They represent aggregated expert knowledge to estimate
84 the broad boundaries of areas where a species is expected to be found (Jetz et al., 2012). They
85 are built using data on the species' evolutionary history, habitat preferences, current occurrences
86 and local knowledge. In many regions, such as the Neotropics, they can represent the only
87 available knowledge of the distribution of a species. However, they only indicate the absence of
88 a species beyond range boundaries, not its exact sites of presence within the range. Further, they
89 contain large spatial and temporal uncertainties, which restricts their usefulness in tracking
90 changes in species distributions over time.

91

92 A new approach to addressing the issues of data incompleteness and heterogeneity is
93 using Integrated Species Distribution Models (ISDMs) (Isaac et al., 2020). ISDMs usually
94 assume that the true but unobserved distribution of a species (the spatial locations of individuals)
95 can be modelled by a Poisson point process conditional on, for instance, environmental
96 covariates. This true distribution can then be sampled through different observation processes,
97 generating the data we observe (presence-absence, presence-only, or abundance). The parameters
98 affecting the intensity of the resulting point pattern can then be estimated using the joint
99 likelihood for the different data types while accounting for the specific ways they were observed.
100 Thus, ISDMs take advantage of the strengths of different data types, and they can also explicitly
101 account for their limitations, like imperfect detection, sampling bias, uneven effort, and varying
102 survey areas (Fletcher Jr. et al., 2019; Miller et al., 2019; Pacifici et al., 2017). Most ISDMs
103 implementations are fitted in a Bayesian framework, which has the advantage of propagating the
104 uncertainties associated with each data type into the predictions and parameter estimates.
105 However, using ISDMs to assess the range dynamics of multiple species at continental scales in
106 regions with limited data availability is still rare (e.g., Grattarola et al., 2023).

107

108 The aim of this study is to model temporal change in the geographic distribution of eight
109 mammal carnivores over the entire Neotropics using a recently developed ISDM (Grattarola et
110 al., 2023). We chose ISDMs because, unlike any other correlative SDM (e.g., MaxEnt), they
111 allow us to integrate different data types, account for varying sample area, sampling intensity and
112 spatial autocorrelation, and include a temporal dimension (Schank et al., 2017). We estimate the
113 geographic range of species in two time periods, 2000-2013 and 2014-2021, quantify the species

114 occupancy changes, and assess the following questions: i) how have species' geographic ranges
115 changed over time, contracted vs. expanded, where and in which direction? ii) how has the
116 species diversity changed? (i.e., species richness) and iii) if dissimilarity among assemblages has
117 decreased (i.e., biotic homogenisation) or increased (i.e., biotic differentiation)?

118

119 **2 Material and methods**

120 We estimated changes in the geographic distribution of species using an ISDM that integrated
121 camera trap survey data with GBIF point occurrences, considered different covariates for each
122 species and accounted for sampling effort and spatial autocorrelation. We quantified the
123 occupancy levels (i.e., probability of occurrence) for each species over time and calculated the
124 beta diversity for each time period and the temporal change in spatial beta diversity.

125

126 **2.1 Species data, observation effort and environmental predictors**

127 The eight species included in the study are the jaguarundi *Herpailurus yagouaroundi* (É.
128 Geoffroy Saint-Hilaire, 1803), ocelot *Leopardus pardalis* (Linnaeus, 1758), margay *Leopardus*
129 *wiedii* (Schinz, 1821), coati *Nasua nasua* (Linnaeus, 1766), crab-eating fox *Cerdocyon thous*
130 (Linnaeus, 1766), maned wolf *Chrysocyon brachyurus* (Illiger, 1815), tayra *Eira barbara*
131 (Linnaeus, 1758), and giant otter *Pteronura brasiliensis* (E. A. W. Zimmermann, 1780). We
132 chose these species because they had sufficient data and no taxonomic issues (e.g., recent
133 taxonomic revision) and to have a balanced representation of the Carnivore biota as they fall
134 under different conservation categories and distribute from south to north of the Neotropics.
135 Based on model performance, we failed to model three of these species (coati, crab-eating fox,
136 and ocelot) and thus they are not included in the posterior analyses (see Results).

137 Since we aimed to compare the distributional change in time, we divided the data into
138 two time periods (time1: 2000-2013 and time2: 2014-2021), the minimum possible to see
139 changes in time given the low number of data points we had for some species (Table 1). The
140 temporal span was chosen considering most of the data available were collected from 2000
141 onwards. The temporal division was chosen to be able to represent, on average, 50% of the data
142 (presence-absence and presence-only) in each period. We expected to have similar uncertainties
143 of distributions due to similar sample sizes in each time period while retaining sufficient data to
144 produce the best estimate of the current distribution without having convergence issues.

145

146

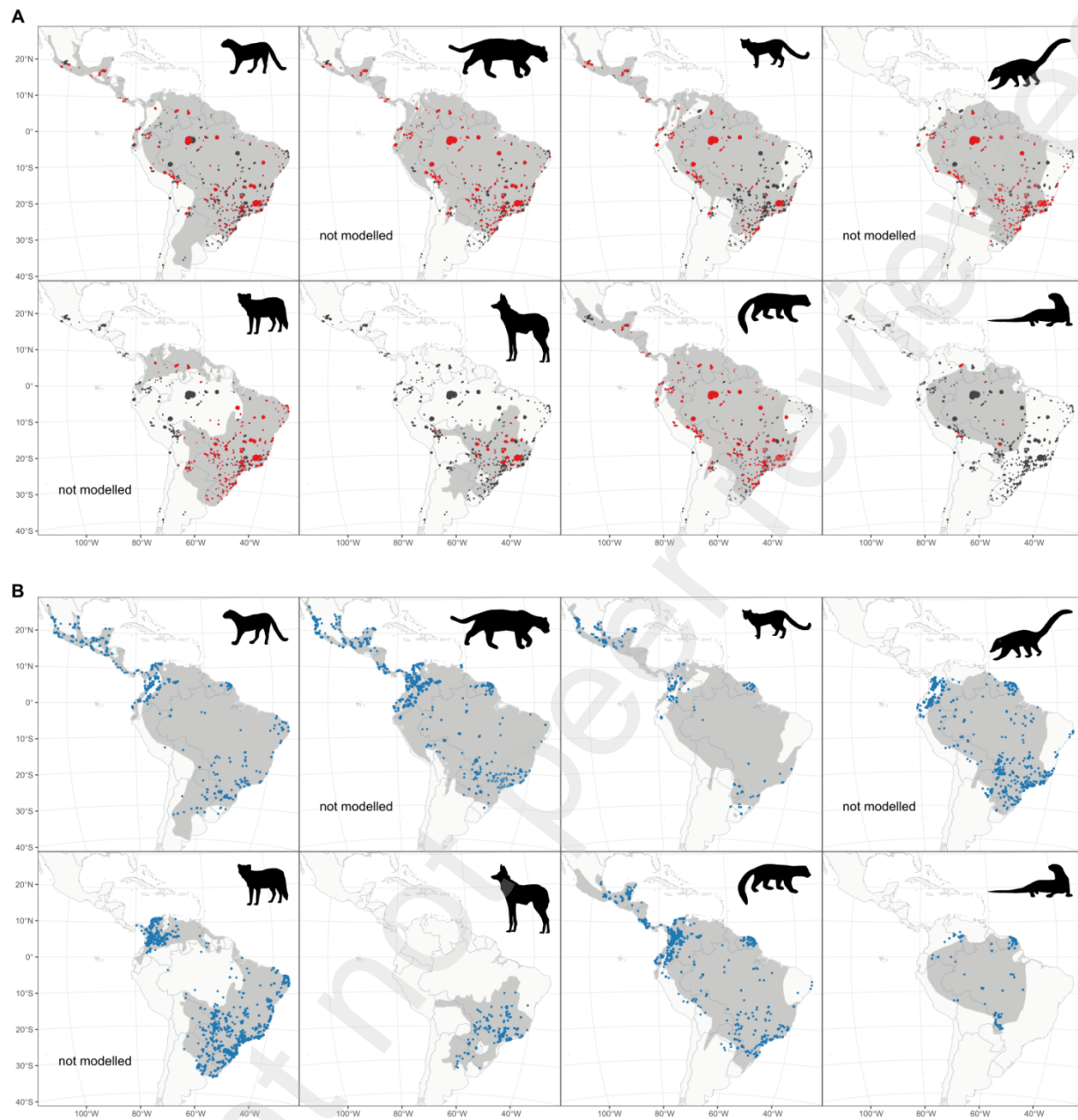
147 **Table 1. Species data.** Presence-only and presence-absence data (in total and by time period), and covariates
 148 used for the eight carnivore species. The IUCN category is shown for each species (LC: least concern, NT:
 149 near threatened, EN: endangered). For an explanation of the covariate abbreviations, see Table A.1.

150

Species	IUCN status	PO data	time1 time2	PA data	time1 time2	covariates
<i>Herpailurus yagouaroundi</i> (jaguarundi)	Least concern (LC)	804	216 588	602	290 312	npp, elevation, bio7, bio15
<i>Leopardus pardalis</i> (ocelot)	Least concern (LC)	2590	378 2212	2963	1584 1379	npp, tree, bio10, bio17
<i>Leopardus wiedii</i> (margay)	Near Threatened (NT)	549	101 448	720	393 327	npp, nontree, bio7, bio10
<i>Nasua nasua</i> (coati)	Least concern (LC)	1978	465 1513	1906	878 1028	nontree, npp, bio10, bio13
<i>Cerdocyon thous</i> (crab-eating fox)	Least concern (LC)	3003	1112 1891	1992	886 1106	urban, tree, bio3, bio4
<i>Chrysocyon brachyurus</i> (maned wolf)	Near Threatened (NT)	475	335 140	386	174 212	elev, grass, bio2, bio14
<i>Eira barbara</i> (tayra)	Least concern (LC)	1740	294 1446	1837	917 920	npp, nontree, bio10, bio17
<i>Pteronura brasiliensis</i> (giant otter)	Endangered (EN)	199	103 96	21	15 6	wetland, woodysavanna, bio3, bio5

151

152



153

154 **Figure 1. Data for the eight carnivore species used in the integrated species distribution model for the**
 155 **entire study period. Top: *Herpailurus yagouaroundi*, *Leopardus pardalis*, *Leopardus wiedii*, and *Nasua***
 156 ***nasua*, and bottom: *Cerdocyon thous*, *Chrysocyon brachyurus*, *Eira barbara*, and *Pteronura brasiliensis*. (A)**
 157 **Presence-absence camera trap data from (Nagy-Reis et al., 2020) and other sources, with presences in red and**
 158 **absences in dark grey. (B) Presence-only point observations from (GBIF.org, 2023) are shown in blue. The**
 159 **IUCN expert map is shown in light grey for each species (IUCN, 2023). The ISDM models of *Leopardus***

160 *pardalis*, *Nasua nasua*, and *Cerdocyon thous* did not converge and thus were not included in the analyses (see
161 Results).

162
163 **Presence-absence data** (Table 1, Figure 1). For all eight species, we extracted these from two
164 workflows: First, we used (Nagy-Reis et al., 2020) database of neotropical carnivores records.
165 We kept camera trap surveys (with detection and non-detection values) with geographic
166 coordinates, information about the study sampling area, starting and ending month and year of
167 the study, and reported the sampling effort (i.e., the number of active camera trap days). To
168 enhance this data source, we collated 32 extra camera trap surveys/datasets considering the same
169 characteristics (see Table A.2 for a complete list of sources). For each survey, we created a
170 buffer polygon using the latitude and longitude of the survey as centroid and either the study area
171 or the latitude/longitude precision for the studies at the sampling level of “area” as the expected
172 area of the polygon (see the metadata in Nagy-Reis et al., 2020 for more details on these
173 definitions). Individual polygons were then overlapped and combined into ‘blobs’ for each time
174 period. Finally, absences were generated for each species in those blobs where the species was
175 not recorded. For each blob, we calculated the total surface area, the time span of the records,
176 and the effort in camera trap days.

177
178
179 **Presence-only data** (Table 1, Figure 1). We downloaded these from GBIF (GBIF.org, 2023),
180 filtering all records with geographic coordinates and no spatial issues for 2000-2021. We further
181 filtered these data by removing records with coordinate precision smaller than three decimal
182 places (i.e., 0.001) and coordinate uncertainty greater than 25,000 m. To these data, we added
183 records from (Nagy-Reis et al., 2020) that were of the type ‘Count data’ and had been surveyed

184 using the following methods: 'Opportunistic', 'Line transect', 'Active searching', 'Roadkill',
185 'Museum'. Finally, we eliminated duplicates considering independent records as individuals
186 recorded on different dates, and latitude and longitude locations. For each time period (time1 and
187 time2), we aggregated the data to 100 x 100 km resolution grid cells (Lambert azimuthal equal-
188 area projection; centre latitude 0° S and centre longitude 73.125° W) covering the entire
189 Neotropics. We chose 100 km as a compromise between computational efficiency and producing
190 meaningful species range descriptions at a continental scale. To account for the uneven sampling
191 effort between both time periods (i.e., more data are shared through GBIF over time), we
192 calculated the ratio of the number of records between time1 and time2, using all the data
193 available in GBIF for the eight species. We found, on average, 27% more records in the second
194 period. This number was used to calibrate the predictions in time2 (see section Model below).

195
196 **Expert range maps.** As an additional source of information, we used expert-drawn IUCN Red
197 List range maps (IUCN, 2023). Although our models (see below) have the flexibility to predict
198 absences in otherwise suitable environments, they may predict (false) presences in unlikely areas
199 for the species. In this context, range maps are an ideal source of information, as they are poor at
200 predicting where exactly a species occurs within the range but reliably identify areas outside of
201 the range where the species is absent. Specifically, we included the distance to the expert range
202 maps in the model (Merow et al., 2016). Most of the IUCN range maps were generated around
203 2010 (2008-2016), so they do not include areas where the species could have recently colonised.
204 To account for this, we used a value of 0 inside the range map (thus, predictions are not affected
205 within the range) and a positive value outside the range given by the distance to the edge of the

206 range map. This is a different approach from Merow et al. (2016), who use range maps as offsets
207 with a fixed pre-defined coefficient, while we estimate that coefficient from the data.

208

209 **Variables describing observation effort.** Thinning variables were used to explain the
210 observation process of the presence-only records (i.e., to adjust the presence-only data for
211 sampling effort). For each 100 x 100 km grid cell, we used data on accessibility from urban areas
212 based on travel time (Weiss et al., 2020) and the country of origin of the record. We expected
213 that highly accessible grid cells would have more point records than inaccessible grid cells and
214 that differences would also vary among countries, as they have different data-sharing capacities
215 and citizen-science levels of participation (Carlen et al., 2024).

216

217 **Environmental predictors.** For both grid cells and blobs, we extracted the 19 bioclimatic
218 variables: elevation (SRTM), land cover, net primary production (NPP), percentage of tree cover
219 and percentage of non-tree vegetation. See Table A.1 for more info about each covariate's
220 source, resolution and time span. Land cover was processed to extract the following classes
221 independently: urban and built-up lands, barren, water bodies, savannas, woody savannas,
222 permanent wetlands, and grasslands. We averaged the yearly values for each covariate over the
223 entire period and used them as a unique layer. Finally, we matched the covariates' data to the
224 presence-only data by averaging values within the 100 x 100 km grid cells and to the presence-
225 absence data by averaging values within blobs.

226

227 One of the features of the Bayesian ISDM is the computational cost and, thus, the near-
228 impossibility to do classical variable selection. To circumvent this problem, we pre-assess the

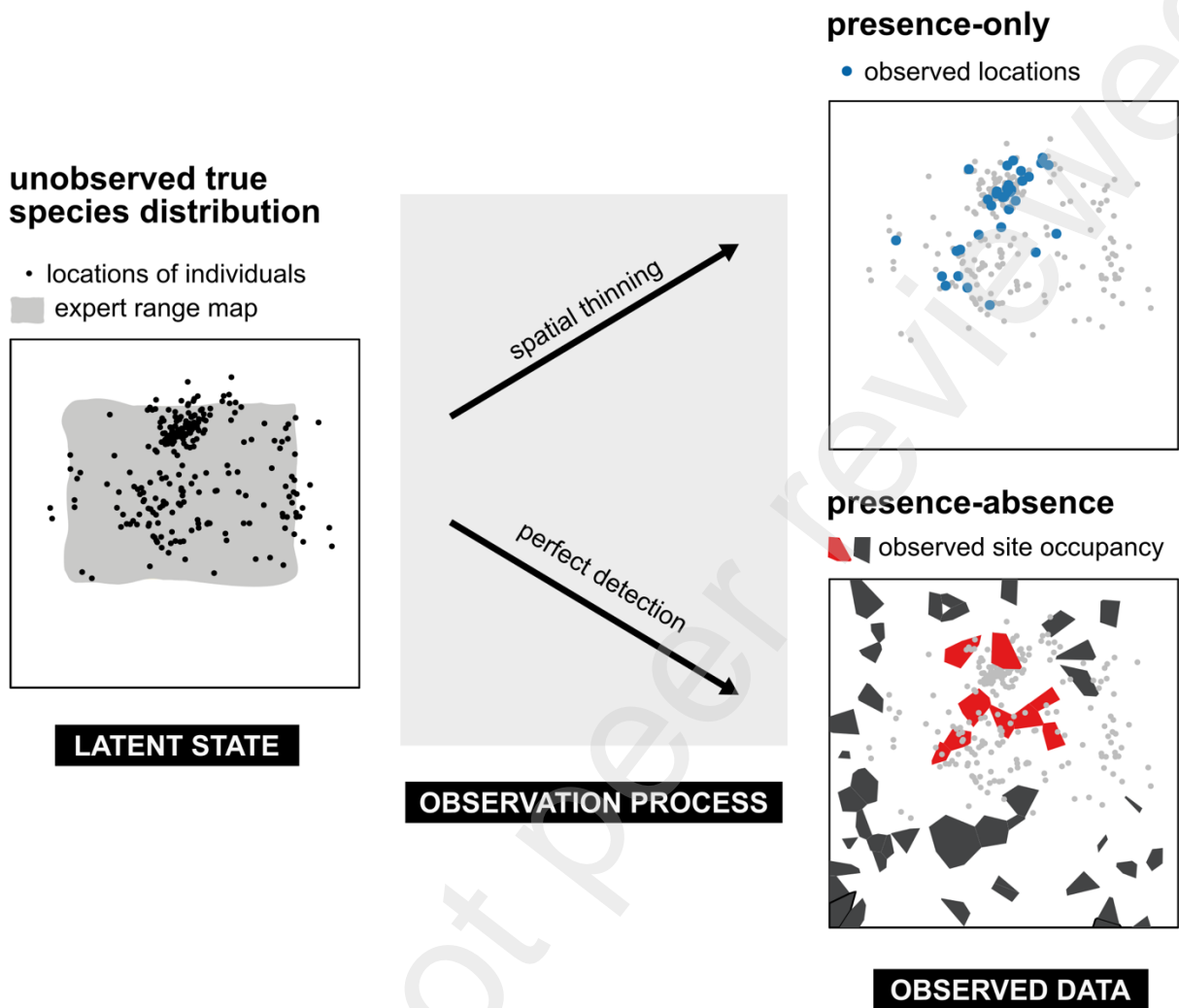
229 potential importance of each environmental predictor for each species using tree-based machine
230 learning analyses (boosted trees, random forests) with the raw presence/absence for both periods
231 combined as a response and all the environmental predictors. Finally, we performed Pearson
232 correlations (r) among the top-selected variables and kept four covariates (aiming at maximum
233 collinearity of $r=0.6$) for each species (Table 1), also taking into account the species preferences
234 based on the available literature: *Herpailurus yagouaroundi* (Caso et al., 2015; de Oliveira,
235 1998a), *Leopardus pardalis* (de Oliveira et al., 2010; Murray & Gardner, 1997), *Leopardus*
236 *wiedii* (de Oliveira, 1998b), *Nasua nasua* (Gompper & Decker, 1998), *Cerdocyon thous*
237 (Machado & Hingst-Zaher, 2009; Tchaicka et al., 2007), *Chrysocyon brachyurus* (Dietz, 1985;
238 Queirolo et al., 2011), *Eira barbara* (Presley, 2000), and *Pteronura brasiliensis* (Noonan et al.,
239 2017).

240

241 **2.2 Model**

242 A full description of the model is available in Appendix B. Here is a short summary: We used an
243 ISDM that combines three different lines of evidence (presence-only, presence-absence data, and
244 expert range maps), accounts for sampling effort and spatial autocorrelation, and has a temporal
245 dimension. Our model (Figure 2) assumes that the true (unobserved) species distribution, i.e., the
246 latent state, is an inhomogeneous Poisson point process conditional on the selected
247 environmental covariates for each species, the distance to the expert range map, spatial splines,
248 and time. This true distribution is then sampled through two different observation processes,
249 generating the presence-only and presence-absence data we see (Figure 2).

250



251

252 **Figure 2. Simplified schematic of the integrated species distribution model (ISDM) used in our study.**

253 The latent state is the true (unobserved) distribution of individuals of the species. It can be modelled by a

254 Poisson point process conditional on environmental covariates, the distance to the expert range map, time, and

255 spatial splines (to account for missing environmental covariates and spatial autocorrelation). This true

256 distribution is then sampled through two different observation processes, generating the presence-only and

257 presence-absence data we observe (shown as blue dots and red and black polygons). The joint likelihood of

258 these observed data, given the unobserved true state and uninformative priors, is then used in MCMC to

259 calculate posterior distributions of the true state.

260

261 We used a similar model to Grattarola et al., (2023). Here, we introduce two novelties: (i)
262 the distance to the edge of the expert map of the species is a covariate in the model, and (ii) we
263 calibrate the estimated number of records per area by the overall sampling effort (measured by
264 the ratio of the number of records between time1 and time2 for all carnivores' data in GBIF).

265

266 **Model evaluation.** We performed posterior predictive checks to evaluate the model's fit (Conn
267 et al., 2018) and plotted expected and observed data to compare them visually. For the PA data,
268 we used AUC (Pearce & Ferrier, 2000) and Tjur's R^2 discrimination coefficient (Tjur, 2009).
269 These values were calculated as part of each model run. For the PO data, we did residual
270 diagnostics using the 'DHARMA' package (Hartig, 2022).

271

272 **2.3 Hotspots of occupancy change**

273 **Quantification.** The area A of the geographic range of a species for each time period ($A_{\text{time}2}$,
274 $A_{\text{time}1}$) was calculated as follows: We first integrated the point pattern intensity over each grid
275 cell to get the expected probability of occurrence in each cell. We then summed these
276 probabilities across all grid cells in the study area. The change of the area of occupancy over
277 time (the number of 100×100 km grid-cells) was calculated as $\Delta A = A_{\text{time}2} - A_{\text{time}1}$. We also
278 calculated the uncertainty of the change (expressed as 95% Bayesian credible intervals) and
279 plotted it in a bivariate plot against the predicted change.

280

281 **Change in species richness.** As each species' models had a different number of iterations, first,
282 we took 1000 samples from the posterior of the occurrence probability for each species in each
283 grid cell and in each time period. Then, we calculated the median probability per species/grid

284 cell, summed the individual predictions at time1 and time2 (i.e., as stacked species distribution
285 models) and finally quantified and mapped the temporal change of species richness between
286 periods in each grid cell.

287
288 **Beta diversity and temporal and spatial dissimilarity.** We calculated (i) beta diversity as the
289 ratio between the total diversity and the average diversity at each grid cell (Anderson et al., 2011;
290 Whittaker, 1960), i.e., as the degree to which regional diversity exceeds local diversity, and we
291 measure it multiplicatively, $\beta_{time} = \gamma / \bar{\alpha}_{time}$, (ii) the spatial variation in temporal dissimilarity
292 for each individual grid cell between the two time periods using Růžička index, and (iii) the
293 temporal change in spatial dissimilarity as the difference in beta-diversity between par of grid
294 cells within the same time period, using Růžička index.

295

296 **2.4 Reproducible workflow**

297 The data were processed in R (R Core Team, 2023). We used the ‘rnatuarearth’ package (South,
298 2017) to obtain Latin American countries’ spatial polygons. Spatial analyses were done using
299 ‘sf’ (Pebesma, 2018) and ‘terra’ (Hijmans, 2022). We downloaded the MODIS data using
300 ‘MODISrsp’ (Busetto & Ranghetti, 2016). The ISDM was run using ‘R2jags’ (Su & Yajima,
301 2020), and the maps were prepared with ‘tmap’ (Tennekes, 2018). Beta diversity was calculated
302 using *vegdist* in ‘vegan’ package (Oksanen et al., 2013). The workflow for each species was split
303 into five Quarto notebooks, including 1) data generation, 2) covariates’ selection, 3) data
304 preparation for modelling, 4) model run, and 4) model outputs. All this is accessible in a GitHub
305 repository at: <https://anonymous.4open.science/r/hotspots-neotropical-carnivores-587A>.

306

307 **3 Results**

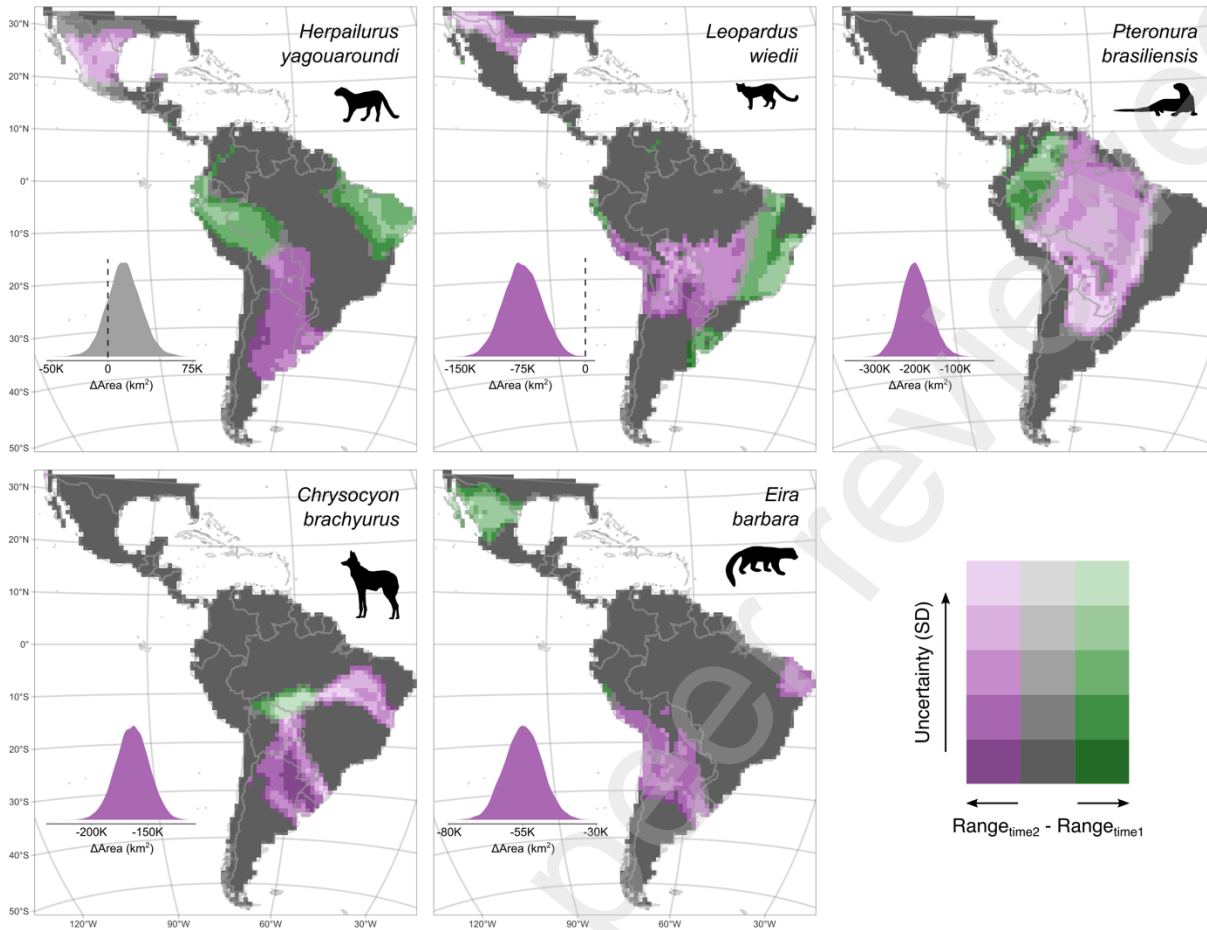
308 We fitted a separate ISDM for each mammal species and revealed their geographic range
309 dynamics in the Neotropics over the last two decades (Figure A.1). Good convergence was
310 reached for all model parameters ($R_{hat} < 1.1$). Of the eight species, five were well supported
311 based on model performance. We were not able to assess the distribution range of *Leopardus*
312 *pardalis*, *Cerdocyon thous*, and *Nasua nasua*. Thus, we excluded this species from the
313 occupancy change analyses. Average Tjur's R^2 was 0.289, and AUC was 0.708 for the PA data
314 (Table A.4), and we saw an overall reasonable fit for the PO data (Figure A.2).

315

316 **3.1 Changes in the area of occupancy of species**

317 The changes in the area of occupancy varied between species, ranging from -2,000,000 km² to
318 146,000 km². They were predominantly negative (Figure 3), meaning that most species (except
319 *Herpailurus yagouaroundi*) decreased their probability of occurrence relative to the initial
320 period.

321



322

323 **Figure 3. Changes in the area of occupancy of species.** The change between the two time periods (2000 to
 324 2013 and 2014 to 2021) is split by the uncertainty of the prediction; darker pink and darker green colours show
 325 highly certain losses and gains, respectively. The distribution of the area of change is shown in the lower left
 326 corner for each species.

327

328 We found that the jaguarundi (*Herpailurus yagouaroundi*) has contracted its southern range
 329 limits in Argentina and south Brazil while maintaining its presence in central Brazil and the
 330 north of South America and expanding its range in the northeast of Brazil (between Cerrado and
 331 Caatinga biomes) and the western Amazon (Figure 3). We saw a non-significant increase in the
 332 species range between the two periods, with a median change in the area of occupancy of

333 146,000 km² (14.6 grid-cells of 100x100km; CI = -22.4, 54.2). The margay (*Leopardus wiedii*)
334 showed range decreases in south Peru and the Chaco and Pantanal regions (Bolivia, Paraguay,
335 north of Argentina and south-western Brazil), and range expansions in the Uruguayan savannah
336 (Uruguay and its borders with Argentina and Brazil), part of Cerrado and Caatinga regions, the
337 north of the Atlantic Forest (Brazil), and the north of Peru and Ecuador. Between both periods,
338 the species contracted its range in -756,000 km² (75.6 grid-cells; CI = -129, -21.1). For the
339 maned wolf (*Chrysocyon brachyurus*), we saw large geographic range contractions that
340 concentrated in the Chaco and Uruguayan savannah regions (Uruguay, north of Argentina, and
341 south Paraguay) and weak expansions over the south-west Amazon moist forests (north Bolivia
342 and south-west Brazil). The median change in the area of occupancy was 1,640,000 km² (164
343 grid-cells; CI = -200, -129). We found that the tayra (*Eira barbara*) has contracted on its
344 southern range limit (central Argentina) and expanded on its northern limit (Mexico). The
345 median decrease in the area of distribution for the tayra was -548,000 km² (54.8 grid-cells; CI = -
346 70.7, -39.4). The giant otter (*Pteronura brasiliensis*) was the species with the largest range loss.
347 Contractions were widespread along the species distribution (mainly in the Amazon basin), with
348 few areas of unchanged areas concentrated in Guiana lowland moist forests and range
349 expansions in the western limits of the species range. The giant otter shrunk its range by a
350 median of 2,000,000 km² (200 grid-cells; CI = -283, -106).

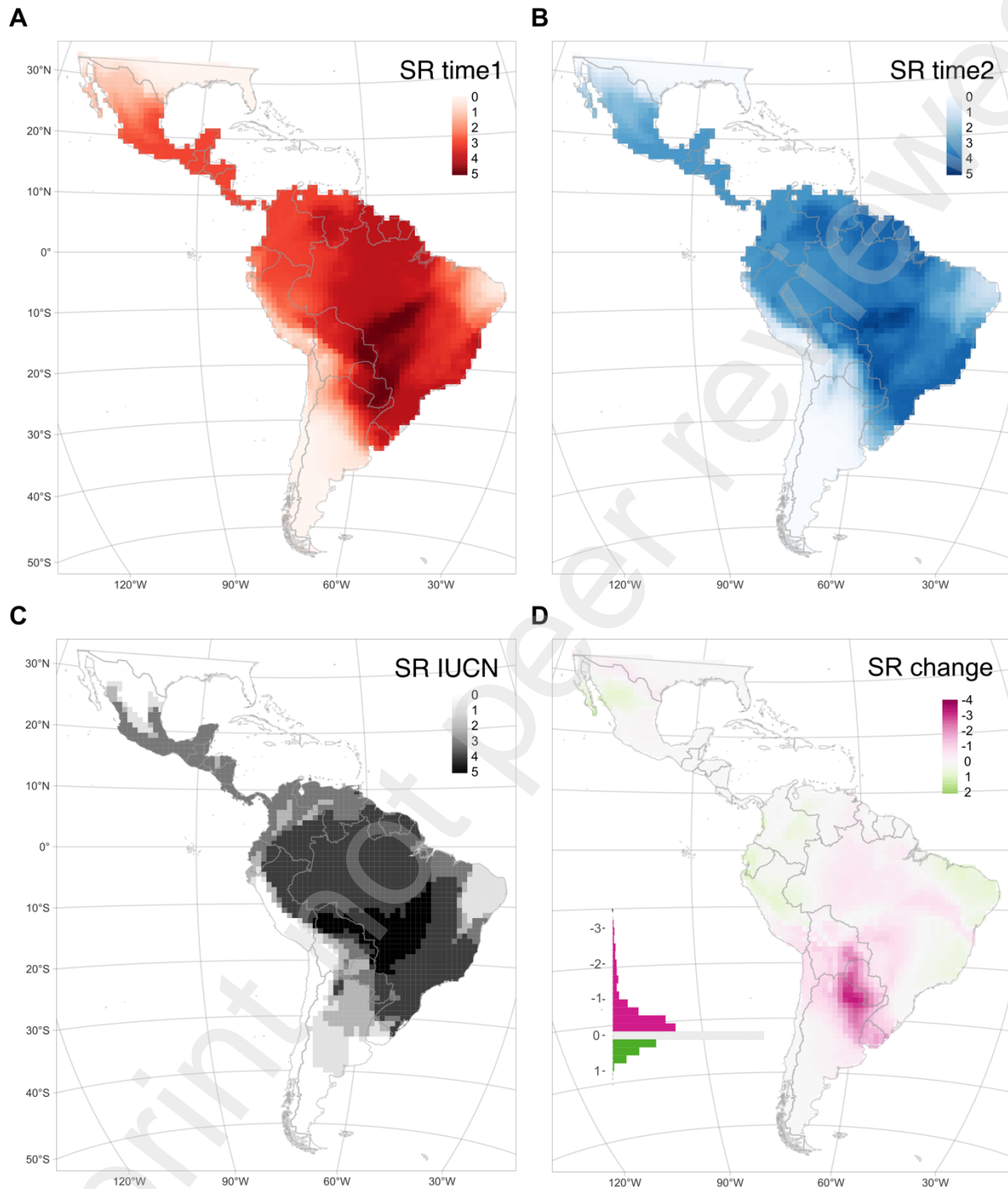
351

352 **3.2 Change in species richness**

353 Species richness at each time period (Figure 4a,b), calculated as the average richness across each
354 period per grid cell, showed an overall similar pattern to that expected by IUCN range maps
355 (Figure 4c). Diversity of the five species peaked between -10 and -25 degrees south and -55 and -

356 35 degrees west and declined towards the west of South America, northeast of Brazil and the
357 north of Mexico. The temporal change in species richness was unevenly distributed across the
358 continent (Figure 4c). Losses were accumulated in a region covering Uruguay, the north of
359 Argentina, Paraguay and south Bolivia, and were mostly driven by the contraction of the ranges
360 of *Chrysocyon brachyurus*, *Herpailurus yagouaroundi*, *Eira barbara*, and *Leopardus wiedii* (see
361 occupancy changes in Figure 3). Gains were less conspicuous and more geographically
362 dispersed, with notable centres in the Caatinga and the Atlantic Forest regions (northeast and
363 southwest of Brazil), the tropical Andes (central and north Peru, west Ecuador and Colombia)
364 and north-west Mexico (Figure 4c).

365



366

367 **Figure 4. Patterns of species richness (SR) and SR change.** Including maned wolf (*Chrysocyon*
 368 *brachyurus*), giant otter (*Pteronura brasiliensis*), jaguarundi (*Herpailurus yagouaroundi*), tayra (*Eira*
 369 *barbara*), and margay (*Leopardus wiedii*). (A) Species richness in time1 (2000 to 2013), (B) species richness

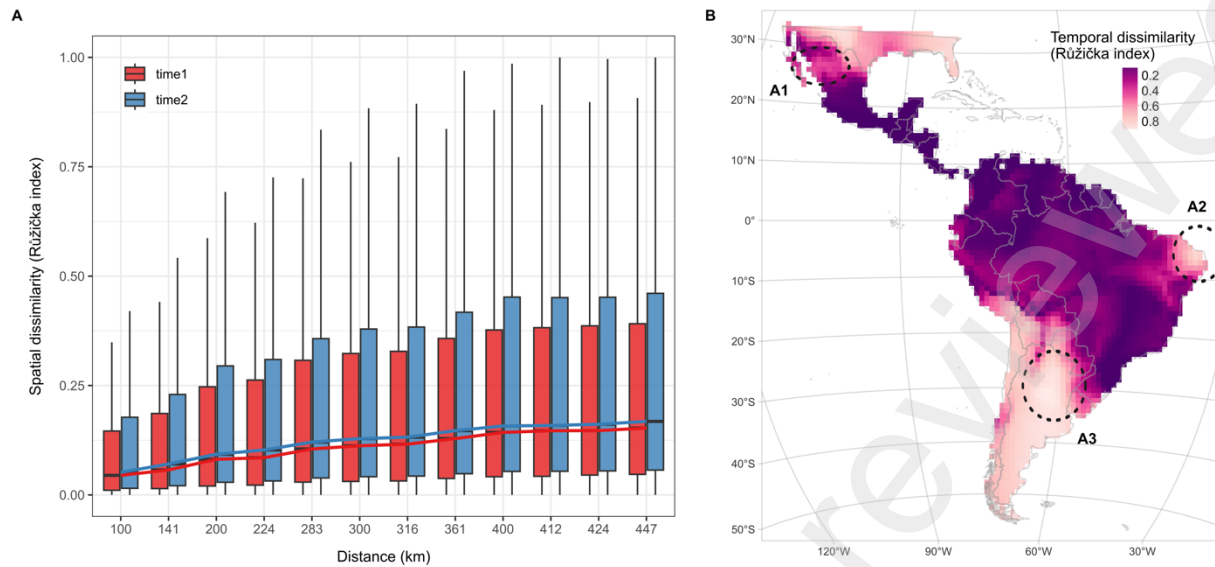
370 in time2 (2014 to 2021), (C) species richness according to the IUCN expert range maps (IUCN, 2023), and (D)
371 change in species richness between both time periods (pink regions indicate species losses and green regions
372 indicate species gains).

373

374 **3.3 Beta diversity and spatial and temporal dissimilarity**

375 Beta diversity, the ratio between the total diversity and the average diversity at each grid cell,
376 increased from $\beta_{time1}=1.911 (\pm 3.321)$ to $\beta_{time2}=2.088 (\pm 3.408)$. We also saw an increase in
377 temporal change of spatial dissimilarity with distance between periods, with time2 being higher
378 than time1 (Figure 5a). Temporal dissimilarity of species composition between time1 and time2,
379 measured by the Růžička index, concentrated around locations with a high concentration of
380 range boundaries (Figure 5b), particularly in the northwest of Mexico (Figure 5b, A1), northeast
381 Brazil (A2), and the northeast of Argentina (A3). The peaks of temporal dissimilarity in Mexico
382 (A1) and Brazil (A2) are also areas of change in species composition. In contrast, the peak in the
383 north of Argentina overlapped the hotspot of species richness loss (Figure 4c). A closer look at
384 the first case (A1) reveals a gain of *Eira barbara* and a loss of *Herpailurus yagouaroundi*, while
385 the second case (A2) is explained by the gain of *Herpailurus yagouaroundi* and the loss of *Eira*
386 *barbara*.

387



388

389 **Figure 5. Change in temporal dissimilarity and spatial dissimilarity of five carnivore species.** Measured
 390 with Růžička index, between 2000-2013 and 2014-2021. (A) Temporal change of spatial dissimilarity, i.e.,
 391 between each time period at the same grid cell. Dissimilarity is higher in time2 and increases with distance for
 392 both periods; time1 is shown in red, and time2 in blue. Lines connecting the median values are also shown. (B)
 393 Spatial variation in temporal dissimilarity, i.e., between pairs of grid cells within the same time period. High
 394 dissimilarity between time1 and time2 is represented in light pink and low in dark purple. A1, A2 and A3
 395 highlight areas of interest due to high dissimilarity and richness (within or on the boundaries of accumulated
 396 species ranges).

397

398

399 **4 Discussion**

400 There is a high demand for empirical assessments of how nature has been changing in response
 401 to anthropogenic pressures. Yet even the most high-profile reports (IPBES, 2019) rely either on
 402 indirect evidence (e.g. habitats degrade and thus biodiversity must decline), on projection
 403 scenarios (e.g. this is how climate changes and biodiversity will follow), or on reports from small
 404 (local) spatial grains (Blowes et al., 2019). In contrast to these, our study provides the first *direct*

405 continent-wide, multi-species and continuous map of hotspots of temporal change in the
406 Neotropics over the last two decades. By focusing on the five carnivores' entire distribution, we
407 identified variations in species' occupancy areas, species richness, and species composition.
408 Most species, one of them listed as endangered and two near threatened (Table 1), underwent
409 range contractions in the last twenty years, their diversity decreased over time, and species
410 composition underwent spatial differentiation (*sensu* Blowes et al., 2022, i.e., dissimilarity
411 among assemblages increased). The type of changes and directions differed among regions and
412 countries, and we suggest that this variation can be linked to the ongoing land use changes in the
413 Neotropical region (Jaureguiberry et al., 2022). Global targets, such as the Kunming-Montreal
414 Global Biodiversity Framework, demand up-to-date biodiversity knowledge to be used for urgent
415 conservation action. Our study provides evidence that shows where and how prominent the
416 declines are in different parts of the continent. Thus, our analysis can contribute to National
417 Biodiversity Assessments and help prioritise areas for immediate conservation action that can be
418 tailored to each species.

419
420 We found the most important changes in three specific areas: west of Mexico (Sierra
421 Madre Occidental and Pacific Lowlands) and northeast of Brazil (Caatinga), with high temporal
422 dissimilarity, and the north of Argentina (Pampa and Chaco), with high dissimilarity and also
423 species loss. The Sierra Madre Occidental tropical dry forest is part of the Mexican transition
424 zone (Morrone, 2017), where the Neotropical and the Nearctic regions overlap. This area has not
425 been the most affected by land use change (González-Abraham et al., 2015), however, drier
426 ecosystems have been disregarded in terms of conservation policies in comparison to tropical
427 evergreen forests in the country (Mendoza-Ponce et al., 2019). This lack of conservation policies

428 could explain the pattern we observe. The Caatinga is the largest tropical dry forest in South
429 America. Although the vegetation in this region is adapted to extreme temperature conditions, it
430 is expected to be highly affected by climate change (Moura, do Nascimento, et al., 2023; Silva et
431 al., 2019). The Caatinga and the Chaco/Pampa regions are not among the biodiversity hotspots of
432 the Neotropics (Myers et al., 2000); they represent areas of medium species richness values.
433 Importantly, these lowland regions have experienced severe land use changes over the last three
434 decades. The Chaco has lost 14.5% of its natural vegetation (1,440,000 km²) compared to 1985,
435 with the greatest loss located in Paraguay (Proyecto Mapbiomas Chaco, 2023), while the Pampa
436 has lost 11.8% (700,000 km²), mainly of native grasslands (Proyecto MapBiomas Pampa
437 Trinacional, 2023; Baeza et al. 2023). The conspicuous species loss in these areas could be a
438 consequence of such profound land use changes.

439
440 We found diverse types of change in each individual species. The *Herpailurus*
441 *yagouaroundi* was the only species that did not experience net declines in its area of occupancy.
442 The disparity between our new findings and previous results, suggesting a slight increase
443 (Grattarola et al., 2023), can be attributed to the incorporation of the species expert range map in
444 our current model. Including this expert-derived information may constrain the predictions,
445 leading to a more accurate representation of the species' actual occupancy dynamics. The
446 increase in the area of occupancy of *H. yagouaroundi* towards the Caatinga region on the border
447 with the Cerrado can be explained by the strong wet/dry climate there, which the jaguarundi
448 prefers (Espinosa et al., 2018). This pattern aligns with (Moura, Oliveira, et al., 2023), who
449 projected an increase in habitat suitability for the species by 2060 there. However, we saw a
450 sharp contraction in the southern limit of its distribution range. Thus, the recent first recordings

451 of the species in Uruguay (Grattarola et al., 2016) could either be an erratic detection of the
452 species or a lack of past sampling effort in the area, but not the expansion of the species.

453

454 In the same area (Uruguayan savannah), we observed an opposite trend for the *Leopardus*
455 *wiedii*, whose occupancy increased over time. Categorized as Near Threatened, *L. wiedii* is
456 highly dependent on trees, and the few forested areas of these grasslands in the region may be
457 key for the species' conservation planning (Espinosa et al., 2018). The main reductions in the
458 area of occupancy for *L. wiedii* were in the west part of the Chaco and the Cerrado, areas
459 characterised by being like savannahs too (i.e., grasslands with a few trees). A key protagonist of
460 the Cerrado is *Chrysocyon brachyurus*, the largest South American canid. *C. brachyurus* is a
461 near-threatened species which showed stable occupancy in this area, yet large declines towards
462 the south of its range, a continuation of a process that had already been documented prior to the
463 year 2000 (Queirolo et al., 2011). *C. brachyurus*, however, has expanded its north-western
464 distribution into the forests of Amazonia. This could be explained by conversions of broad areas
465 of the lower Amazon to livestock pastures (Souza et al., 2020), giving the species larger open
466 areas to occupy.

467

468 The *Eira barbara*'s area of occupancy also declined, in particular, around the species'
469 southern limit and towards the Caatinga in northeast Brazil, aligning with the projected range
470 shifts of (Moura, Oliveira, et al., 2023). *E. barbara*'s area of occupancy in the centre of Mexico
471 showed an increase, although the species is uncommon there and considered endangered in the
472 whole country. The recent range expansions documented in south and central Mexico could,
473 however, support our findings (García et al., 2016; Ruiz-Gutiérrez et al., 2017). Finally,

474 *Pteronura brasiliensis*, one of the most endangered mammals of the Neotropics (Noonan et al.,
475 2017), was the species with the most prominent declines in the area of occupancy, with few areas
476 of expansion that were located in the upper Amazon. There is evidence that *P. brasiliensis* may
477 be recovering in this area, around north Perú and northeastern Ecuadorian Amazon (Groenendijk
478 et al., 2014), but there are also reports of population declines in western Colombia and south
479 Perú and within the rest of the entire range (Groenendijk et al., 2022). Critically, most
480 populations of *P. brasiliensis* are fragmented and isolated. Despite slowly recovering from
481 decades of hunting for the pelt trade, deforestation of the Amazon and contamination of water
482 bodies (e.g., by mining) are, in any case, making the species more vulnerable (Brum et al., 2021).

483

484 The presence-absence data we used are more evenly spread than presence-only data, and both
485 data types are spatially complementary. Therefore, they jointly present low imbalances in the
486 geographic space they cover. However, a question may arise whether the estimated occupancy
487 change is real and not a mere reflection of survey effort. Here are the reasons why the latter is
488 unlikely: (1) our predicted ranges align with the current expert knowledge (IUCN range) and not
489 with the perceived imbalance in the raw data, (2) we account for several facets of the effort in the
490 model, and (3) since the model is Bayesian, an area with insufficient data translates in high
491 prediction uncertainty, which we then report.

492 We show that the model of *Herpailurus yagouaroundi* originally developed by Grattarola
493 et al., (2023) can incorporate expert range maps and be applied to four other carnivore species;
494 however, we were not able to fit it for three species, *Leopardus pardalis*, *Cerdocyon thous*, and
495 *Nasua nasua*, because the model showed poor residual diagnostics fit (Figure A.2). This may be
496 because they are widespread habitat generalists that do not respond to our broad-scale

497 environmental covariates or exhibit a clear spatially structured trend. Still, classical model
498 performance metrics such as AUC and R^2 are difficult to interpret in hierarchical models that
499 incorporate both observation and process sub-models (including ISDMs and occupancy models
500 as described by MacKenzie et al., 2018). These metrics should not be applied in the same way as
501 in classical SDMs. The challenge arises because the model estimates the unobserved true
502 occupancy, which represents the actual occupancy, assuming the model is correct. Consequently,
503 the only valid dataset for calculating AUC and R^2 would need to accurately reflect this
504 unobserved true occupancy, demanding data from sites where every individual is detected and
505 identified. Such comprehensive data are practically unattainable. Even though the analysis of
506 trends in the remaining five species may seem limited, it still represents the first example of how
507 temporal changes of occupancy and diversity can be scaled up to entire ranges and multiple
508 species with limited and heterogeneous data. This highlights the potential of ISDMs to
509 understand how biodiversity changes over time.

510 In all, we put a temporal perspective on the continental-wide distributions of carnivore
511 species in the Neotropics and discussed potential drivers of change. We unveiled the species'
512 large-scale range dynamics, a key step to implementing conservation measures at the local scale.
513 With this temporal multi-species approach, we have paved the way to a dynamic macroecology
514 which no longer produces static range polygons or maps from species distribution models.
515 Instead, we envision a scenario where field guides, or information signs in zoological gardens,
516 come with both contemporary and historical distributions. This is necessary in order to grasp the
517 full extent of the ongoing global biodiversity change, particularly for the general public.

518

519 **5 Acknowledgements**

520 We are grateful to Diana Bowler and Bob O’Hara for their valuable advice. Silhouettes by
521 Gabriela Palomo-Muñoz (CC BY-NC) and Margot Michaud (CC0) - PhyloPic. FG and PK were
522 funded by the European Union (ERC, BEAST, 101044740). Views and opinions expressed are,
523 however, those of the author(s) only and do not necessarily reflect those of the European Union
524 or the European Research Council Executive Agency. Neither the European Union nor the
525 granting authority can be held responsible for them.

526

527 **6 Author contributions**

528 Florencia Grattarola: conceptualization (equal); data curation (lead); formal analysis (lead);
529 investigation (lead); methodology (equal); visualisation (lead); writing – original draft (equal);
530 writing – review and editing (equal). Kateřina Tschernostrová: data curation (supporting);
531 writing – review and editing (supporting). Petr Keil: conceptualization (equal); formal analysis
532 (supporting); funding acquisition (lead); investigation (supporting); methodology (equal); writing
533 – original draft (equal); writing – review and editing (equal).

534

535 **7 Funding**

536 European Union (ERC, BEAST, 101044740).

537

538 **8 Data Accessibility Statement**

539 The data used for this study are openly available at Nagy-Reis et al., (2020)

540 (<https://doi.org/10.1002/ecy.3128>) and GBIF.org, (2023)

541 (<https://doi.org/10.15468/DL.TVVZDQ>). A list of the additional sources gathered for this study

542 can be seen in Table A.2. To see the code for all the analyses and the workflow followed for
543 each species, including data preparation, covariates selection, model run and model outputs,
544 access our GitHub repository: [https://anonymous.4open.science/r/hotspots-neotropical-](https://anonymous.4open.science/r/hotspots-neotropical-carnivores-587A)
545 [carnivores-587A](https://anonymous.4open.science/r/hotspots-neotropical-carnivores-587A).

546

547 **9 References**

- 548 Ahumada, J. A., Silva, C. E. F., Gajapersad, K., Hallam, C., Hurtado, J., Martin, E., McWilliam, A., Mugerwa, B.,
549 O'Brien, T., Rovero, F., Sheil, D., Spironello, W. R., Winarni, N., & Andelman, S. J. (2011). Community
550 structure and diversity of tropical forest mammals: Data from a global camera trap network. *Philosophical*
551 *Transactions of the Royal Society B: Biological Sciences*, 366(1578), 2703–2711.
552 <https://doi.org/10.1098/rstb.2011.0115>
- 553 Anderson, M. J., Crist, T. O., Chase, J. M., Vellend, M., Inouye, B. D., Freestone, A. L., Sanders, N. J., Cornell, H.
554 V., Comita, L. S., Davies, K. F., Harrison, S. P., Kraft, N. J. B., Stegen, J. C., & Swenson, N. G. (2011).
555 Navigating the multiple meanings of β diversity: A roadmap for the practicing ecologist. *Ecology Letters*,
556 14(1), 19–28. <https://doi.org/10.1111/j.1461-0248.2010.01552.x>
- 557 Baeza, S., Vélez-Martin, E., De Abelleira, D., Banchero, S., Gallego, F., Schirmbeck, J., Veron, S., Vallejos, M.,
558 Weber, E., Oyarzabal, M., Barbieri, A., Petek, M., Guerra Lara, M., Sarraillhé, S. S., Baldi, G., Bagnato, C.,
559 Bruzzone, L., Ramos, S., & Hasenack, H. (2022). Two decades of land cover mapping in the Río de la
560 Plata grassland region: The MapBiomias Pampa initiative. *Remote Sensing Applications: Society and*
561 *Environment*, 28, 100834. <https://doi.org/10.1016/j.rsase.2022.100834>
- 562 Barlow, J., França, F., Gardner, T. A., Hicks, C. C., Lennox, G. D., Berenguer, E., Castello, L., Economo, E. P.,
563 Ferreira, J., Guénard, B., Gontijo Leal, C., Isaac, V., Lees, A. C., Parr, C. L., Wilson, S. K., Young, P. J., &
564 Graham, N. A. J. (2018). The future of hyperdiverse tropical ecosystems. *Nature*, 559(7715), Article 7715.
565 <https://doi.org/10.1038/s41586-018-0301-1>
- 566 Blowes, S. A., McGill, B., Brambilla, V., Chow, C. F. Y., Engel, T., Fontrodona-Eslava, A., Martins, I. S., McGlenn,
567 D., Moyes, F., Sagouis, A., Shimadzu, H., Klink, R. van, Xu, W.-B., Gotelli, N. J., Magurran, A., Dornelas,

568 M., & Chase, J. M. (2022). Synthesis reveals biotic homogenisation and differentiation are both common.
569 *bioRxiv*, 2022.07.05.498812. <https://doi.org/10.1101/2022.07.05.498812>

570 Blowes, S. A., Supp, S. R., Antão, L. H., Bates, A., Bruelheide, H., Chase, J. M., Moyes, F., Magurran, A., McGill,
571 B., Myers-Smith, I. H., Winter, M., Bjorkman, A. D., Bowler, D. E., Byrnes, J. E. K., Gonzalez, A., Hines,
572 J., Isbell, F., Jones, H. P., Navarro, L. M., ... Dornelas, M. (2019). The geography of biodiversity change in
573 marine and terrestrial assemblages. *Science*, 366(6463), 339–345. <https://doi.org/10.1126/science.aaw1620>

574 Bogoni, J. A., Peres, C. A., & Ferraz, K. M. P. M. B. (2020). Extent, intensity and drivers of mammal defaunation:
575 A continental-scale analysis across the Neotropics. *Scientific Reports*, 10(1), Article 1.
576 <https://doi.org/10.1038/s41598-020-72010-w>

577 Brown, J. H., Stevens, G. C., & Kaufman, D. M. (1996). THE GEOGRAPHIC RANGE: Size, Shape, Boundaries,
578 and Internal Structure. *Annual Review of Ecology and Systematics*, 27(1), 597–623.
579 <https://doi.org/10.1146/annurev.ecolsys.27.1.597>

580 Brum, S., Rosas-Ribeiro, P., Amaral, R. de S., Souza, D. A. de, Castello, L., & Silva, V. M. F. da. (2021).
581 Conservation of Amazonian aquatic mammals. *Aquatic Conservation: Marine and Freshwater Ecosystems*,
582 31(5), 1068–1086. <https://doi.org/10.1002/aqc.3590>

583 Busetto, L., & Ranghetti, L. (2016). MODISstp: An R package for preprocessing of MODIS Land Products time
584 series. *Computers & Geosciences*, 97, 40–48. <https://doi.org/10.1016/j.cageo.2016.08.020>

585 Carlen, E. J., Estien, C. O., Caspi, T., Perkins, D., Goldstein, B. R., Kreling, S. E. S., Hentati, Y., Williams, T. D.,
586 Stanton, L. A., Des Roches, S., Johnson, R. F., Young, A. N., Cooper, C. B., & Schell, C. J. (2024). A
587 framework for contextualizing social-ecological biases in contributory science data. *People and Nature*,
588 6(2), 377–390. <https://doi.org/10.1002/pan3.10592>

589 Caso, A., de Oliveira, T., & Carvajal, S. (2015). *Herpailurus yagouaroundi*. *The IUCN Red List of Threatened*
590 *Species 2015: E.T9948A50653167* (p. 13). <https://www.iucnredlist.org/species/pdf/50653167>

591 Coelho, M. T. P., Barreto, E., Rangel, T. F., Diniz-Filho, J. A. F., Wüest, R. O., Bach, W., Skeels, A., McFadden, I.
592 R., Roberts, D. W., Pellissier, L., Zimmermann, N. E., & Graham, C. H. (2023). The geography of climate
593 and the global patterns of species diversity. *Nature*, 622(7983), Article 7983.
594 <https://doi.org/10.1038/s41586-023-06577-5>

595 Conn, P. B., Johnson, D. S., Williams, P. J., Melin, S. R., & Hooten, M. B. (2018). A guide to Bayesian model
596 checking for ecologists. *Ecological Monographs*, 88(4), 526–542. <https://doi.org/10.1002/ecm.1314>

597 Curtis, P. G., Slay, C. M., Harris, N. L., Tyukavina, A., & Hansen, M. C. (2018). Classifying drivers of global forest
598 loss. *Science*, 361(6407), 1108–1111. <https://doi.org/10.1126/science.aau3445>

599 de Oliveira, T. G. (1998a). *Herpailurus yagouaroundi*. *Mammalian Species*, 578, 1–6.
600 <https://doi.org/10.2307/3504500>

601 de Oliveira, T. G. (1998b). *Leopardus wiedii*. *Mammalian Species*, 579, 1–6. <https://doi.org/10.2307/3504400>

602 de Oliveira, T. G., Tortato, M. A., Silveira, L., Kasper, C. B., Mazim, F. D., Lucherini, M., Jácomo, A. T., Soares, J.
603 B. G., Marques, R. V., & Sunquist, M. (2010). Ocelot ecology and its effect on the small-felid guild in the
604 lowland neotropics. In *The biology and conservation of wild felids* (pp. 559–580). Oxford University Press.

605 Delisle, Z. J., Flaherty, E. A., Nobbe, M. R., Wzientek, C. M., & Swihart, R. K. (2021). Next-Generation Camera
606 Trapping: Systematic Review of Historic Trends Suggests Keys to Expanded Research Applications in
607 Ecology and Conservation. *Frontiers in Ecology and Evolution*, 9.
608 <https://www.frontiersin.org/articles/10.3389/fevo.2021.617996>

609 Dietz, J. M. (1985). *Chrysocyon brachyurus*. *Mammalian Species*, 234, 1–4. <https://doi.org/10.2307/3503796>

610 Emer, C., Galetti, M., Pizo, M. A., Jordano, P., & Verdú, M. (2019). Defaunation precipitates the extinction of
611 evolutionarily distinct interactions in the Anthropocene. *Science Advances*, 5(6), eaav6699.
612 <https://doi.org/10.1126/sciadv.aav6699>

613 Espinosa, C. C., Trigo, T. C., Tirelli, F. P., da Silva, L. G., Eizirik, E., Queirolo, D., Mazim, F. D., Peters, F. B.,
614 Favarini, M. O., & de Freitas, T. R. O. (2018). Geographic distribution modeling of the margay (*Leopardus*
615 *wiedii*) and jaguarundi (*Puma yagouaroundi*): A comparative assessment. *Journal of Mammalogy*, 99(1),
616 252–262. <https://doi.org/10.1093/jmammal/gyx152>

617 Fletcher Jr., R. J., Hefley, T. J., Robertson, E. P., Zuckerberg, B., McCleery, R. A., & Dorazio, R. M. (2019). A
618 practical guide for combining data to model species distributions. *Ecology*, 100(6), e02710.
619 <https://doi.org/10.1002/ecy.2710>

620 García, J. J. M., García, A. D. M., & Cruz, J. M. C. (2016). Registros del Tayra (*Eira barbara* Linneanus 1758) en el
621 estado de Hidalgo, México. *Revista Mexicana de Mastozoología (Nueva Época)*, 6(1), Article 1.
622 <https://doi.org/10.22201/ie.20074484e.2016.6.1.218>

623 Gaston, K. J. (2003). *The structure and dynamics of geographic ranges*. Oxford University Press on Demand.

624 GBIF.org. (2023). *Occurrence Download—Carnivores from the Neotropical region* [Dataset]. The Global
625 Biodiversity Information Facility. <https://doi.org/10.15468/DL.TVVZDQ>

626 Gompper, M. E., & Decker, D. M. (1998). *Nasua nasua*. *Mammalian Species*, 580, 1–9.
627 <https://doi.org/10.2307/3504444>

628 González-Abraham, C., Ezcurra, E., Garcillán, P. P., Ortega-Rubio, A., Kolb, M., & Creel, J. E. B. (2015). The
629 Human Footprint in Mexico: Physical Geography and Historical Legacies. *PLOS ONE*, 10(3), e0121203.
630 <https://doi.org/10.1371/journal.pone.0121203>

631 Grattarola, F., Bowler, D. E., & Keil, P. (2023). Integrating presence-only and presence–absence data to model
632 changes in species geographic ranges: An example in the Neotropics. *Journal of Biogeography*, 50(9),
633 1561–1575. <https://doi.org/10.1111/jbi.14622>

634 Grattarola, F., Hernández, D., Duarte, A., Gaucher, L., Perazza, G., González, S., Bergós, L., Chouhy, M., Garay,
635 A., & Carabio, M. (2016). Primer registro de yaguarundí (*Puma yagouarundi*) (Mammalia: Carnivora:
636 Felidae) en Uruguay, con comentarios sobre monitoreo participativo. *Boletín de La Sociedad Zoológica Del*
637 *Uruguay*, 25, 85–91. http://journal.szu.org.uy/index.php/Bol_SZU/article/view/23

638 Grenyer, R., Orme, C. D., Jackson, S. F., Thomas, G. H., Davies, R. G., Davies, T. J., Jones, K. E., Olson, V. A.,
639 Ridgely, R. S., Rasmussen, P. C., Ding, T. S., Bennett, P. M., Blackburn, T. M., Gaston, K. J., Gittleman, J.
640 L., & Owens, I. P. (2006). Global distribution and conservation of rare and threatened vertebrates. *Nature*,
641 444(7115), 93–96. <https://doi.org/10.1038/nature05237>

642 Groenendijk, J., Hajek, F., Johnson, P. J., Macdonald, D. W., Calvimontes, J., Staib, E., & Schenck, C. (2014).
643 Demography of the Giant Otter (*Pteronura brasiliensis*) in Manu National Park, South-Eastern Peru:
644 Implications for Conservation. *PLOS ONE*, 9(8), e106202. <https://doi.org/10.1371/journal.pone.0106202>

645 Groenendijk, J., Leuchtenberger, C., Marmontel, M., Damme, P. V., Wallace, R. B., & Schenck, C. (2022).
646 *Pteronura brasiliensis* (amended version of 2021 assessment) (The IUCN Red List of Threatened Species).
647 <https://dx.doi.org/10.2305/IUCN.UK.2022-2.RLTS.T18711A222719180.en>

648 Hartig, F. (2022). *DHARMA: Residual Diagnostics for Hierarchical (Multi-Level / Mixed) Regression Models*.
649 <https://CRAN.R-project.org/package=DHARMA>

650 Hijmans, R. J. (2022). *terra: Spatial Data Analysis* (1.5-21) [Computer software]. [https://CRAN.R-](https://CRAN.R-project.org/package=terra)
651 [project.org/package=terra](https://CRAN.R-project.org/package=terra)

652 Hortal, J., Bello, F. de, Diniz-Filho, J. A. F., Lewinsohn, T. M., Lobo, J. M., & Ladle, R. J. (2015). Seven Shortfalls
653 that Beset Large-Scale Knowledge of Biodiversity. *Annual Review of Ecology, Evolution, and Systematics*,
654 *46*(1), 523–549. <https://doi.org/10.1146/annurev-ecolsys-112414-054400>

655 IPBES. (2019). *Summary for policymakers of the global assessment report on biodiversity and ecosystem services of*
656 *the Intergovernmental Science-Policy Platform on Biodiversity and Ecosystem Services* (p. 56). IPBES
657 Secretariat. <https://doi.org/10.5281/zenodo.3553579>

658 Isaac, N. J. B., Jarzyna, M. A., Keil, P., Dambly, L. I., Boersch-Supan, P. H., Browning, E., Freeman, S. N.,
659 Golding, N., Guillera-Arroita, G., Henrys, P. A., Jarvis, S., Lahoz-Monfort, J., Pagel, J., Pescott, O. L.,
660 Schmucki, R., Simmonds, E. G., & O’Hara, R. B. (2020). Data Integration for Large-Scale Models of
661 Species Distributions. *Trends in Ecology & Evolution*, *35*(1), 56–67.
662 <https://doi.org/10.1016/j.tree.2019.08.006>

663 IUCN. (2023). *The IUCN Red List of Threatened Species*. <http://www.iucnredlist.org>

664 Jaureguiberry, P., Titeux, N., Wiemers, M., Bowler, D. E., Coscieme, L., Golden, A. S., Guerra, C. A., Jacob, U.,
665 Takahashi, Y., Settele, J., Díaz, S., Molnár, Z., & Purvis, A. (2022). The direct drivers of recent global
666 anthropogenic biodiversity loss. *Science Advances*, *8*(45), eabm9982.
667 <https://doi.org/10.1126/sciadv.abm9982>

668 Jetz, W., McPherson, J. M., & Guralnick, R. P. (2012). Integrating biodiversity distribution knowledge: Toward a
669 global map of life. *Trends in Ecology & Evolution*, *27*(3), 151–159.
670 <https://doi.org/10.1016/j.tree.2011.09.007>

671 Kissling, W. D., Ahumada, J. A., Bowser, A., Fernandez, M., Fernández, N., García, E. A., Guralnick, R. P., Isaac,
672 N. J. B., Kelling, S., Los, W., McRae, L., Mihoub, J.-B., Obst, M., Santamaria, M., Skidmore, A. K.,
673 Williams, K. J., Agosti, D., Amariles, D., Arvanitidis, C., ... Hardisty, A. R. (2018). Building essential
674 biodiversity variables (EBVs) of species distribution and abundance at a global scale. *Biological Reviews*,
675 *93*(1), 600–625. <https://doi.org/10.1111/brv.12359>

676 Koleff, P., Gaston, K. J., & Lennon, J. J. (2003). Measuring beta diversity for presence–absence data. *Journal of*
677 *Animal Ecology*, *72*(3), 367–382. <https://doi.org/10.1046/j.1365-2656.2003.00710.x>

678 Kühl, H. S., Bowler, D. E., Bösch, L., Bruelheide, H., Dauber, J., Eichenberg, D., Eisenhauer, N., Fernández, N.,
679 Guerra, C. A., Henle, K., Herbing, I., Isaac, N. J. B., Jansen, F., König-Ries, B., Kühn, I., Nilsen, E. B.,
680 Pe'er, G., Richter, A., Schulte, R., ... Bonn, A. (2020). Effective Biodiversity Monitoring Needs a Culture
681 of Integration. *One Earth*, 3(4), 462–474. <https://doi.org/10.1016/j.oneear.2020.09.010>

682 Machado, F. de A., & Hingst-Zaher, E. (2009). Investigating South American biogeographic history using patterns
683 of skull shape variation on *Cerdocyon thous* (Mammalia: Canidae). *Biological Journal of the Linnean*
684 *Society*, 98(1), 77–84. <https://doi.org/10.1111/j.1095-8312.2009.01274.x>

685 MacKenzie, D. I., Nichols, J. D., Royle, J. A., Pollock, K. H., Bailey, L. L., & Hines, J. E. (Eds.). (2018).
686 *Occupancy Estimation and Modeling (Second Edition)*. Academic Press. [https://doi.org/10.1016/B978-0-](https://doi.org/10.1016/B978-0-12-407197-1.00023-5)
687 [12-407197-1.00023-5](https://doi.org/10.1016/B978-0-12-407197-1.00023-5)

688 Magioli, M., Ferraz, K. M. P. M. de B., Chiarello, A. G., Galetti, M., Setz, E. Z. F., Paglia, A. P., Abrego, N.,
689 Ribeiro, M. C., & Ovaskainen, O. (2021). Land-use changes lead to functional loss of terrestrial mammals
690 in a Neotropical rainforest. *Perspectives in Ecology and Conservation*, 19(2), 161–170.
691 <https://doi.org/10.1016/j.pecon.2021.02.006>

692 Mendoza-Ponce, A., Corona-Núñez, R. O., Galicia, L., & Kraxner, F. (2019). Identifying hotspots of land use cover
693 change under socioeconomic and climate change scenarios in Mexico. *Ambio*, 48(4), 336–349.
694 <https://doi.org/10.1007/s13280-018-1085-0>

695 Merow, C., Wilson, A. M., & Jetz, W. (2016). Integrating occurrence data and expert maps for improved species
696 range predictions. *Global Ecology and Biogeography*, 26(2), 243–258. <https://doi.org/10.1111/geb.12539>

697 Miller, D. A. W., Pacifici, K., Sanderlin, J. S., & Reich, B. J. (2019). The recent past and promising future for data
698 integration methods to estimate species' distributions. *Methods in Ecology and Evolution*, 10(1), 22–37.
699 <https://doi.org/10.1111/2041-210X.13110>

700 Mittermeier, R. A., Turner, W. R., Larsen, F. W., Brooks, T. M., & Gascon, C. (2011). *Global Biodiversity*
701 *Conservation: The Critical Role of Hotspots*. 3–22. https://doi.org/10.1007/978-3-642-20992-5_1

702 Morrone, J. J. (2017). *Neotropical Biogeography. Regionalization and Evolution*. CRC Press.
703 <https://doi.org/10.1201/b21824>

704 Moura, M. R., do Nascimento, F. A. O., Paolucci, L. N., Silva, D. P., & Santos, B. A. (2023). Pervasive impacts of
705 climate change on the woodiness and ecological generalism of dry forest plant assemblages. *Journal of*
706 *Ecology*, *111*(8), 1762–1776. <https://doi.org/10.1111/1365-2745.14139>

707 Moura, M. R., Oliveira, G. A., Paglia, A. P., Pires, M. M., & Santos, B. A. (2023). Climate change should drive
708 mammal defaunation in tropical dry forests. *Global Change Biology*, *29*(24), 6931–6944.
709 <https://doi.org/10.1111/gcb.16979>

710 Murray, J. L., & Gardner, G. L. (1997). *Leopardus pardalis*. *Mammalian Species*, *548*, 1–10.
711 <https://doi.org/10.2307/3504082>

712 Myers, N., Mittermeier, R. A., Mittermeier, C. G., Da Fonseca, G. A., & Kent, J. (2000). Biodiversity hotspots for
713 conservation priorities. *Nature*, *403*(6772), 853. <https://doi.org/10.1038/35002501>

714 Nagy-Reis, M., Oshima, J. E. de F., Kanda, C. Z., Palmeira, F. B. L., de Melo, F. R., Morato, R. G., Bonjorne, L.,
715 Magioli, M., Leuchtenberger, C., Rohe, F., Lemos, F. G., Martello, F., Alves-Eigenheer, M., da Silva, R.
716 A., Silveira dos Santos, J., Priante, C. F., Bernardo, R., Rogeri, P., Assis, J. C., ... Ribeiro, M. C. (2020).
717 NEOTROPICAL CARNIVORES: a data set on carnivore distribution in the Neotropics. *Ecology*, *101*(11),
718 e03128. <https://doi.org/10.1002/ecy.3128>

719 Noonan, P., Prout, S., & Hayssen, V. (2017). *Pteronura brasiliensis* (Carnivora: Mustelidae). *Mammalian Species*,
720 *49*(953), 97–108. <https://doi.org/10.1093/mspecies/sex012>

721 Oksanen, J., Blanchet, F. G., Kindt, R., Legendre, P., Minchin, P. R., O'hara, R., Simpson, G. L., Solymos, P.,
722 Stevens, M. H. H., & Wagner, H. (2013). Package 'vegan.' *Community Ecology Package, Version*, *2*(9).

723 Oliveira, U., Paglia, A. P., Brescovit, A. D., de Carvalho, C. J., Silva, D. P., Rezende, D. T., Leite, F. S. F., Batista,
724 J. A. N., Barbosa, J. P. P., & Stehmann, J. R. (2016). The strong influence of collection bias on
725 biodiversity knowledge shortfalls of Brazilian terrestrial biodiversity. *Diversity and Distributions*, *22*(12),
726 1232–1244. <https://doi.org/10.1111/ddi.12489>

727 Pacifici, K., Reich, B. J., Miller, D. A. W., Gardner, B., Stauffer, G., Singh, S., McKerrow, A., & Collazo, J. A.
728 (2017). Integrating multiple data sources in species distribution modeling: A framework for data fusion*.
729 *Ecology*, *98*(3), 840–850. <https://doi.org/10.1002/ecy.1710>

730 Pearce, J., & Ferrier, S. (2000). Evaluating the predictive performance of habitat models developed using logistic
731 regression. *Ecological Modelling*, *133*(3), 225–245. [https://doi.org/10.1016/S0304-3800\(00\)00322-7](https://doi.org/10.1016/S0304-3800(00)00322-7)

732 Pebesma, E. (2018). Simple Features for R: Standardized Support for Spatial Vector Data. *The R Journal*, 10(1),
733 439–446. <https://doi.org/10.32614/RJ-2018-009>

734 Pocock, M. J. O., Chandler, M., Bonney, R., Thornhill, I., Albin, A., August, T., Bachman, S., Brown, P. M. J.,
735 Cunha, D. G. F., Grez, A., Jackson, C., Peters, M., Rabarijaon, N. R., Roy, H. E., Zaviero, T., & Danielsen,
736 F. (2018). Chapter Six—A Vision for Global Biodiversity Monitoring With Citizen Science. In D. A.
737 Bohan, A. J. Dumbrell, G. Woodward, & M. Jackson (Eds.), *Advances in Ecological Research* (Vol. 59,
738 pp. 169–223). Academic Press. <https://doi.org/10.1016/bs.aecr.2018.06.003>

739 Pompeu, J., Assis, T. O., & Ometto, J. P. (2023). Landscape changes in the Cerrado: Challenges of land clearing,
740 fragmentation and land tenure for biological conservation. *Science of The Total Environment*, 167581.
741 <https://doi.org/10.1016/j.scitotenv.2023.167581>

742 Presley, S. J. (2000). Eira barbara. *Mammalian Species*, 2000(636), 1–6. [https://doi.org/10.1644/1545-1410\(2000\)636<0001:EB>2.0.CO;2](https://doi.org/10.1644/1545-1410(2000)636<0001:EB>2.0.CO;2)

744 Queirolo, D., Moreira, J. R., Soler, L., Emmons, L. H., Rodrigues, F. H. G., Pautasso, A. A., Cartes, J. L., &
745 Salvatori, V. (2011). Historical and current range of the Near Threatened maned wolf *Chrysocyon*
746 *brachyurus* in South America. *Oryx*, 45(2), 296–303. <https://doi.org/10.1017/S0030605310000372>

747 R Core Team. (2023). *R: A Language and Environment for Statistical Computing* [Computer software]. R
748 Foundation for Statistical Computing. <https://www.R-project.org/>

749 Raven, P. H., Gereau, R. E., Phillipson, P. B., Chatelain, C., Jenkins, C. N., & Ulloa Ulloa, C. (2020). The
750 distribution of biodiversity richness in the tropics. *Science Advances*, 6(37), eabc6228.
751 <https://doi.org/10.1126/sciadv.abc6228>

752 Roll, U., Feldman, A., Novosolov, M., Allison, A., Bauer, A. M., Bernard, R., Bohm, M., Castro-Herrera, F., Chirio,
753 L., Collen, B., Colli, G. R., Dabool, L., Das, I., Doan, T. M., Grismer, L. L., Hoogmoed, M., Itescu, Y.,
754 Kraus, F., LeBreton, M., ... Meiri, S. (2017). The global distribution of tetrapods reveals a need for
755 targeted reptile conservation. *Nat Ecol Evol*, 1(11), 1677–1682. <https://doi.org/10.1038/s41559-017-0332-2>

756 Ruiz-Gutiérrez, F., Vázquez-Arroyo, E., & Chávez, C. (2017). Range Expansion of a Locally Endangered Mustelid
757 (Eira barbara) in Southern Mexico. *Western North American Naturalist*, 77(3), 408–413.
758 <https://doi.org/10.3398/064.077.0301>

759 Sandom, C., Faurby, S., Sandel, B., & Svenning, J.-C. (2014). Global late Quaternary megafauna extinctions linked
760 to humans, not climate change. *Proceedings of the Royal Society B: Biological Sciences*, 281(1787),
761 20133254. <https://doi.org/10.1098/rspb.2013.3254>

762 Schank, C. J., Cove, M. V., Kelly, M. J., Mendoza, E., O’Farrill, G., Reyna-Hurtado, R., Meyer, N., Jordan, C. A.,
763 González-Maya, J. F., Lizcano, D. J., Moreno, R., Dobbins, M. T., Montalvo, V., Sáenz-Bolaños, C.,
764 Jimenez, E. C., Estrada, N., Cruz Díaz, J. C., Saenz, J., Spínola, M., ... Miller, J. A. (2017). Using a novel
765 model approach to assess the distribution and conservation status of the endangered Baird’s tapir. *Diversity*
766 *and Distributions*, 23(12), 1459–1471. <https://doi.org/10.1111/ddi.12631>

767 Schipper, J., Chanson, J. S., Chiozza, F., Cox, N. A., Hoffmann, M., Katariya, V., Lamoreux, J., Rodrigues, A. S. L.,
768 Stuart, S. N., Temple, H. J., Baillie, J., Boitani, L., Lacher, T. E., Mittermeier, R. A., Smith, A. T.,
769 Absolon, D., Aguiar, J. M., Amori, G., Bakkour, N., ... Young, B. E. (2008). The Status of the World’s
770 Land and Marine Mammals: Diversity, Threat, and Knowledge. *Science*, 322(5899), 225–230.
771 <https://doi.org/10.1126/science.1165115>

772 Scotson, L., Johnston, L. R., Iannarilli, F., Wearn, O. R., Mohd-Azlan, J., Wong, W. M., Gray, T. N. E., Dinata, Y.,
773 Suzuki, A., Willard, C. E., Frechette, J., Loken, B., Steinmetz, R., Moßbrucker, A. M., Clements, G. R., &
774 Fieberg, J. (2017). Best practices and software for the management and sharing of camera trap data for
775 small and large scales studies. *Remote Sensing in Ecology and Conservation*, 3(3), 158–172.
776 <https://doi.org/10.1002/rse2.54>

777 Silva, J. L. S. e, Cruz-Neto, O., Peres, C. A., Tabarelli, M., & Lopes, A. V. (2019). Climate change will reduce
778 suitable Caatinga dry forest habitat for endemic plants with disproportionate impacts on specialized
779 reproductive strategies. *PLOS ONE*, 14(5), e0217028. <https://doi.org/10.1371/journal.pone.0217028>

780 Song, X.-P., Hansen, M. C., Potapov, P., Adusei, B., Pickering, J., Adami, M., Lima, A., Zalles, V., Stehman, S. V.,
781 Di Bella, C. M., Conde, M. C., Copati, E. J., Fernandes, L. B., Hernandez-Serna, A., Jantz, S. M., Pickens,
782 A. H., Turubanova, S., & Tyukavina, A. (2021). Massive soybean expansion in South America since 2000
783 and implications for conservation. *Nature Sustainability*, 4(9), 784–792. [https://doi.org/10.1038/s41893-](https://doi.org/10.1038/s41893-021-00729-z)
784 [021-00729-z](https://doi.org/10.1038/s41893-021-00729-z)

785 South, A. (2017). *rnaturalearth: World Map Data from Natural Earth (0.1.0)* [Computer software].
786 <https://CRAN.R-project.org/package=rnaturalearth>

787 Souza, C. M., Z. Shimbo, J., Rosa, M. R., Parente, L. L., A. Alencar, A., Rudorff, B. F. T., Hasenack, H.,
788 Matsumoto, M., G. Ferreira, L., Souza-Filho, P. W. M., de Oliveira, S. W., Rocha, W. F., Fonseca, A. V.,
789 Marques, C. B., Diniz, C. G., Costa, D., Monteiro, D., Rosa, E. R., Vélez-Martin, E., ... Azevedo, T.
790 (2020). Reconstructing Three Decades of Land Use and Land Cover Changes in Brazilian Biomes with
791 Landsat Archive and Earth Engine. *Remote Sensing*, 12(17), Article 17. <https://doi.org/10.3390/rs12172735>
792 Steenweg, R., Hebblewhite, M., Kays, R., Ahumada, J., Fisher, J. T., Burton, C., Townsend, S. E., Carbone, C.,
793 Rowcliffe, J. M., Whittington, J., Brodie, J., Royle, J. A., Switalski, A., Clevenger, A. P., Heim, N., &
794 Rich, L. N. (2017). Scaling-up camera traps: Monitoring the planet's biodiversity with networks of remote
795 sensors. *Frontiers in Ecology and the Environment*, 15(1), 26–34. <https://doi.org/10.1002/fee.1448>
796 Su, Y.-S., & Yajima, M. (2020). *R2jags: Using R to Run "JAGS."* <https://CRAN.R-project.org/package=R2jags>
797 Tchaicka, L., Eizirik, E., De Oliveira, T. G., Cândido Jr, J. F., & Freitas, T. R. O. (2007). Phylogeography and
798 population history of the crab-eating fox (*Cerdocyon thous*). *Molecular Ecology*, 16(4), 819–838.
799 <https://doi.org/10.1111/j.1365-294X.2006.03185.x>
800 Tennekes, M. (2018). tmap: Thematic Maps in R. *Journal of Statistical Software*, 84(6), 1–39.
801 <https://doi.org/10.18637/jss.v084.i06>
802 Tjur, T. (2009). Coefficients of Determination in Logistic Regression Models—A New Proposal: The Coefficient of
803 Discrimination. *The American Statistician*, 63(4), 366–372. <https://doi.org/10.1198/tast.2009.08210>
804 Whittaker, R. H. (1960). Vegetation of the Siskiyou Mountains, Oregon and California. *Ecological Monographs*,
805 30(3), 279–338. <https://doi.org/10.2307/1943563>
806 WWF. (2020). *Living Planet Report 2020—Bending the curve of biodiversity loss*.
807